

A Novel ICD Coding Framework Based on Associated and Hierarchical Code Description Distillation

First Author

Bin Zhang

Tongji University, Shanghai, China
2233009@tongji.edu.cn

Second Author

Junli Wang

Tongji University, Shanghai, China
junliwang@tongji.edu.cn

Abstract

ICD(International Classification of Diseases) coding involves assigning ICD codes to patients visit based on their medical notes. ICD coding is a challenging multilabel text classification problem due to noisy medical document inputs. Recent advancements in automated ICD coding have enhanced performance by integrating additional data and knowledge bases with the encoding of medical notes and codes. However, most of them ignore the code hierarchy, leading to improper code assignments. To address these problems, we propose a novel framework based on associated and hierarchical code description distillation (AHDD) for better code representation learning and avoidance of improper code assignment. we utilize the code description and the hierarchical structure inherent to the ICD codes. Therefore, in this paper, we leverage the code description and the hierarchical structure inherent to the ICD codes. The code description is also applied to aware the attention layer and output layer. Experimental results on the benchmark dataset show the superiority of the proposed framework over several state-of-the-art baselines.

1 Introduction

The International Classification of Diseases (ICD), overseen by the World Health Organization, is a key coding system in healthcare, assigning codes to diagnostic and procedural data from patient visits. These codes standardize and systemize health information globally, aiding in epidemiological studies, service billing, and health trend monitoring (Tsui, 2002; Bottle and Aylin, 2008; Choi et al., 2016). However, the manual nature of ICD coding presents significant challenges, including the training of medical experts and the difficulty of accurately assigning codes from a large set, as seen in the ICD-9 and ICD-10's extensive code lists. This manual process is costly, time-consuming, and prone to errors (O'Malley et al., 2005), sparking

Medical Note The patient was taken for an ERCP the day after admission, where he was found to have a stone in the common bile duct treated with sphincterotomy and stone extraction. He was treated with broad spectrum antibiotics. Following the ERCP, he then appeared to bleed from his sphincterotomy. His initial hematocrit was 40 and it then fell to 25. He received 2 units of transfusion . He was then stable after that.
Parent code:285 Description:Other and unspecified anemias
ICD-9 code:285.1 Description:Acute posthemorrhagic anemia
Sibling code:285.8 Description:Other specified anemias

Figure 1: An example of a medical note annotated with ICD-9 code "285.1", its parent code "285", and the sibling code "285.8". The words highlighted in red represent terms found in the descriptions of the child codes, aiding in the identification of key words within the medical note. Conversely, the words in blue denote terms that differ from the sibling code's description, serving to pinpoint more closely related words, thereby enhancing accuracy.

growing interest in automated ICD coding in both industry and academia.

Viewing medical code prediction as a multi-label text classification challenge, a variety of machine learning-based methods have been developed and proposed. These include rule-based (Medori and Fairon, 2010), Support Vector Machine (SVM)-based (Perotte et al., 2014), and decision tree-based methods (Scheurwegs et al., 2017). With the advent of deep learning in NLP tasks, a significant focus has been placed on learning deep representations of medical notes. This has been achieved using Recurrent Neural Networks (RNNs) (Vu et al., 2020; Yuan et al., 2022), Convolutional Neural Networks (CNNs) (Mullenbach et al., 2018; Li and Yu, 2020), or Transformer (Luo et al., 2021) encoders, followed by multi-label classification for code pre-

diction. Advanced state-of-the-art methods utilize a label attention mechanism to pinpoint representative words in medical notes and words with higher weights are then used as significant evidence for making predictions (Chen et al., 2023; Gomes et al., 2024),.

Although effective, those methods do not target at the noisy text in medical note. Noisy text problem indicates that medical notes are lengthy and noisy, where only some key phrases are highly related to the coding task. Medical notes, typically authored by doctors and nurses, exhibit a range of writing styles. It is pointed out in (Zhou et al., 2021) that approximately 10% of words in a medical note are pertinent to the task of code assignment. These parts are not only redundant but can also be misleading in the context of ICD coding. Training models with such noisy text can lead to confusion about where to attention and result in erroneous decisions due to semantic deviations.

To address the noisy text problem, a self-distillation learning mechanism is proposed to ensure the extracted shared representations focus on the long medical note’s important part (Zhou et al., 2021; Luo et al., 2024). However, these methods overlook the code hierarchy, leading to improper code assignments, as the child codes of a parent are very similar clinically. To tackle this problem, we focus on the code descriptions and the hierarchical structure inherent to the ICD codes. Each ICD code typically comes with a concise description, and they are organized in a hierarchical manner. For example, as illustrated in Figure 1, both ICD code 285.1 (Acute posthemorrhagic anemia) and ICD code 285.8 (Other specified anemias) are the children of ICD code 285 (Other and unspecified anemias). We can effectively identify key terms related to "anemia" in code description, including "initial hematocrit", "fell" and "transfusion". These descriptions helps to streamline and clarify lengthy, noisy medical notes. However, since ICD code 285.1 and 285.8 are more clinically relevant, the model possibly assign both codes to a medical code. According to (Xie and Xing, 2018; Wang et al., 2023), it is unlikely to simultaneously assign all children codes of a parent to a medical code. To prevent inappropriate code assignments, we also capture important word "bleed" in the document by the word "acute posthemorrhagic" in code description different from sibling code.

Therefore, in this paper, we propose a novel framework based on associated and hierarchical

code description distillation to predict ICD codes. Specifically, the medical note, associated code and hierarchical code are fed into the shared encoder. We apply code description aware attention mechanism to get the label-specific representation. Then both associated code and hierarchical code applied to distill the medical note. Finally the code description aware output is applied for classification. The experimental results demonstrate that our proposed framework surpasses several leading state-of-the-art models on a benchmark dataset.

The principal contributions of this paper are as follows:

- A novel framework based on associated and hierarchical code description distillation (AHDD) is proposed to predict ICD codes. The code description is also applied to aware the attention layer and output layer. To the best of our knowledge, our work is the first attempt to use associated and hierarchical code descriptions for distilling medical notes.
- The framework is encoder-agnostic. And it neither needs extra text processing nor brings in too many parameters. Experimental results with a benchmark dataset demonstrate the effectiveness of the proposed framework.
- The extensive experiments about noisy text demonstrate that our proposed framework can identifying key words within noisy and lengthy medical notes.

2 Related Work

ICD coding has been a significant task garnering attention for decades. Medori and Fairon (2010) utilized a rule-based methodology to extract essential snippets from medical notes, encoding them with ICD codes. Perotte et al. (2014) introduced an SVM classifier employing bag-of-words features. Scheurwegs et al. (2017) attempted to identify key features using a decision tree-based approach. However, these methods did not attain satisfactory performance, primarily due to the challenge of extracting useful features from the complex and noisy medical notes.

With the popularity of neural networks, many researchers focused on using RNN CNN and Transformer models for ICD coding. (Li and Yu, 2020) used convolutional layers with different kernel sizes to extract relevant information for each code from source medical notes. (Vu et al., 2020) concentrated on identifying label-specific words in

notes using an LSTM equipped with a custom label attention mechanism. (Biswas et al., 2021) was the first to propose a Transformer-based approach, achieving results on par with CNN-based models.

To further improve the performance, incorporating code descriptions and external knowledge had been explored. (Zhou et al., 2021) trained a teacher network informed by label descriptions and modeled code co-occurrence using interactive shared attention. (Yuan et al., 2022; Wang et al., 2023; Xie et al., 2024) harnessed code synonyms from a medical knowledge graph, adapting a multi-head attention mechanism. (Wang et al., 2022) integrated external Wikipedia knowledge and implemented a medical concept-driven attention. But all of them ignore the code hierarchy, which easily leads to improper code assignments.

In terms of code hierarchy, (Cao et al., 2020) proposed a hyperbolic representation method to leverage the code hierarchy. (Vu et al., 2020; Chen et al., 2023; Luo et al., 2024), introduced a hierarchical joint learning architecture, considering the hierarchical relationships among codes. However, these methods just use code hierarchy in output layer to avoid inappropriate code assignments. It is insufficient to capture the key words in medical note. Contrarily, we utilize the associated and hierarchical code description to capture the key word by distillation.

3 Methods

ICD Coding: ICD coding represents a complex task of multi-label classification. Specifically, consider a medical note composed of N_d tokens:

$$d = \{t_1, t_2, \dots, t_{N_d}\}, \quad (1)$$

and the medical code set $L = \{l_1, l_2, \dots, l_{N_L}\}$, where the size is denoted by N_L . Additionally, each medical code is accompanied by a brief description, represented as $c_i = \{t_1^c, t_2^c, \dots, t_{N_{c_i}}^c\}$, where N_{c_i} signifies the length of the code’s description and $i \in [1, N_L]$.

The multi-label classification is transformed into binary classification, where the objective is to assign a binary label $l_i \in \{0, 1\}$ to each ICD code within the label space L . Here, the label 1 indicates a positive association with an ICD-identified disease or procedure.

The overall architecture of the proposed framework (AHDD) is shown in Figure 2, which consists of four parts: (1) Encoder Layer which generates

the hidden state of the medical notes and code description; (2) Code Description Aware Attention which computes the label-specific document representation; (3) Associated and Hierarchical Code Description Distillation which distills the noisy medical notes with the aid of the associated codes and their sibling codes’ description; (4) Code Description Aware Output which predicts the medical codes.

3.1 Encoder Layer

Initially, we transform each word into a compact, low-dimensional word embedding. Specifically, each token t_i in a document d is represented by a corresponding pre-trained word embedding x_i , each sharing a uniform embedding size.

In terms of the encoder, theoretically, it can be implemented using any type of neural encoder, such as CNN based encoders (Mullenbach et al., 2018; Li and Yu, 2020), RNN based encoders (Vu et al., 2020; Yuan et al., 2022) or Transformer based encoders (Luo et al., 2021). For a given medical note embeddings $X_d = \{x_1, x_2, \dots, x_{N_d}\}$, the encoder generates a hidden state for each word. The encoder processes these word embeddings to produce text hidden representations $H_d = \{h_1, h_2, \dots, h_{N_d}\} \in \mathbb{R}^{N_d \times h}$, where h denotes the dimensionality of the hidden state.

$$H_d = \text{Enc}(x_1, x_2, \dots, x_{N_d}) \quad (2)$$

3.2 Code Description Aware Attention

In medical notes, not every word contributes equally to medical diagnosis decision-making. Thus, attention weights are employed to refine medical note representations in alignment with code description representations.

Previous studies (Li and Yu, 2020; Vu et al., 2020) have used H_d as input to compute N_L label-specific representations. This process involves two steps. Initially, a label-wise attention weight matrix α is calculated as follows:

$$\text{Attention}(Q, K, V) = \text{softmax}(QK^T)V \quad (3)$$

$$\alpha = \text{Attention}(U, H_d, H_d) \quad (4)$$

This phase involves learning code-dependent parameters $U \in \mathbb{R}^{N_L \times h}$ for the attention weights. However, the attention for rare codes may not be effectively learned due to limited training data. To address this, we compute the value of each code description’s hidden representations using the same

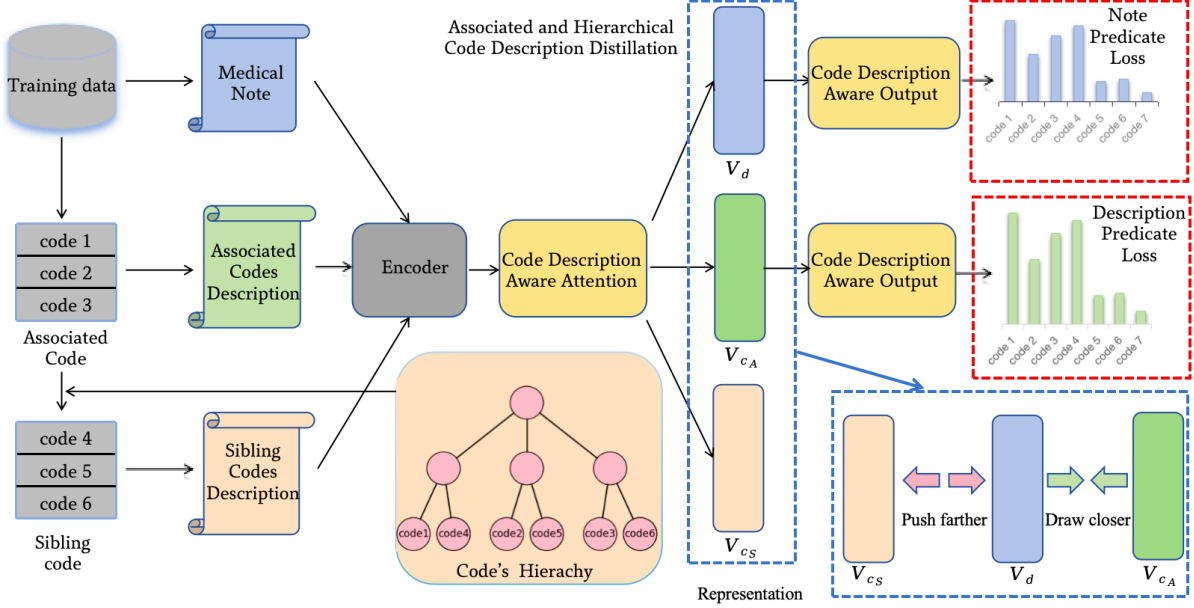


Figure 2: The architecture of proposed **AHDD** framework. V_d , V_{c_A} , and V_{c_S} represent the label-specific representation for the medical note, associated code, and sibling code, respectively. It is important to highlight that the Backbone Encoder can be implemented using various neural encoders.

encoder, followed by a max-pooling operation to generate the code's representations H_i^c . Subsequently, we concatenate these code's representations to form H_C . This matrix H_C undergoes a linear projection to substitute for U . The only parameters required for learning are the linear projection parameters $W_Q \in \mathbb{R}^{h \times h}$.

$$H_i^c = \text{MaxPool}(\text{Enc}(x_1^c, x_2^c, \dots, x_{N_{c_i}}^c)) \quad (5)$$

$$H_C = \{H_1^c, H_2^c, \dots, H_{N_i}^c\} \quad (6)$$

$$\alpha_C = \text{Attention}(H_C W_Q, H_d, H_d) \quad (7)$$

Then, the matrix α_C is applied to calculate a weighted sum of H_d , creating the label-specific document representation:

$$V_d = H_d \cdot \alpha_C \quad (8)$$

3.3 Associated and Hierarchical Code Description Distillation

To deal with the long and noisy text in ICD coding task, we use the associated codes' description to distill the medical note, effectively sifting through and removing irrelevant words from the medical note. Furthermore, to ensure the capture of medical terms that are specifically relevant to a given label and distinct from similar sibling codes, we incorporate the descriptions of these sibling codes in our distillation. This distillation is crucial in removing words that are more closely related to the sibling codes rather than the associated code.

3.3.1 Associated Code Description Distillation

Given a medical note d and its associated code set L_A , we consider the set of these associated codes' description $c_A = \{c_1, c_2, \dots, c_{N_{L_A}}\}$ as critical for classification. Here, N_{L_A} represents the size of the associated code set L_A . We aim to get the information relevant to the associated code by distilling the medical note. Specially, we align the label-specific representations of the medical note closer to those of the associated codes' descriptions, treating the latter as training data for classification.

The label-specific document representation V_{c_A} of the associated codes' descriptions is obtained using the same encoder and attention layer. We measure the similarity between V_{c_A} and V_d using cosine distance, striving to minimize this distance.

$$\cos(V_d, V_{c_A}) = \frac{1}{N_L} \sum_{i=1}^{N_L} \frac{V_d^i \cdot V_{c_A}^i}{\|V_d^i\| \|V_{c_A}^i\|} \quad (9)$$

$$L_{sim} = 1 - \cos(V_d, V_{c_A}) \quad (10)$$

where, V_d^i denotes the document representations for the i_{th} label.

The loss for associated code descriptions distillation comprises two components: the similarity between V_{c_A} and V_d , and the binary cross-entropy loss using associated codes' descriptions as training

data.

$$\text{Loss}(c_A, y) = - \sum_{i=1}^{N_L} (y_i \log \bar{y}_i^A + (1-y_i)(1-\log \bar{y}_i^A)) \quad (11)$$

$$L_{ades} = \lambda_{sim} \cdot L_{sim} + \text{Loss}(c_A, y) \quad (12)$$

where, y is the target label and \bar{y}^A is the predicted label with the input of associated codes' description c_A .

3.3.2 Hierarchical Code Description Distillation

ICD codes are structured in a tree-like hierarchy, reflecting parent-child and sibling relationships. Upper-level nodes signify broader disease categories, while lower-level nodes detail specific diseases. This hierarchy helps identify mutually exclusive codes. For instance, if codes X and Y are siblings under Z, it's improbable for both to be assigned to a patient concurrently. However, the sibling codes are more clinically relevant.

To effectively harness this hierarchical structure and ensure the accurate capture of medical terms that are relevant to a specific label and distinguishable from those associated with similar sibling codes, we utilize a distillation by the hierarchical code description. More specifically, we aim to differentiate the label-specific representation within a medical note from the descriptions pertinent to its sibling codes.

The loss for hierarchical code description distillation is the dissimilarity between the label-specific document representation of medical note V_d and sibling codes' descriptions V_{c_S} , striving to maximize the dissimilarity. The dissimilarity between V_d and V_{c_S} is quantified similarly to the aforementioned similarity measure:

$$\cos(V_d, V_{c_S}) = \frac{1}{N_L} \sum_{i=1}^{N_L} \frac{V_d^i \cdot V_{c_S}^i}{\|V_d^i\| \|V_{c_S}^i\|} \quad (13)$$

$$L_{dis} = \cos(V_d, V_{c_S}) \quad (14)$$

$$L_{sdes} = \lambda_{dis} \cdot L_{dis} \quad (15)$$

where, c_S denotes the description of sibling codes, and V_{c_S} represents the label-specific representation of the sibling codes' description c_S .

3.4 Code Description Aware Output

For each label-specific representation V_d , we determine whether the medical note \mathbf{d} contains the code

l_i by evaluating the similarity between the code's and medical note's representations.

In previous works (Li and Yu, 2020; Luo et al., 2021), the label-specific representation V_d is fed into a linear layer, followed by a sum-pooling operation to generate the score vector \hat{y}^d for all ICD codes. Subsequently, the probability vector \bar{y}^d is derived using the sigmoid function.

$$\hat{y}^d = \text{SumPool}(V_d W) \quad (16)$$

$$\bar{y}^d = \text{sigmoid}(\hat{y}^d) \quad (17)$$

where, the code-dependent parameter matrix $W \in \mathbb{R}^{h \times N_L}$ must be learned for classification. However, due to imbalanced data distribution, learning the weight matrix W can be challenging. To address this, we have incorporate the similarity between the code's and medical note's representations. Specially, we calculate W^C , derived from all code descriptions' hidden representations, and then passed through a linear layer. Then we use $V_d W^C + V_d W$ in place of the original $V_d W$ to focus more intensely on those rare codes.

$$W^C = (H^C W^l)^T, \quad W^l \in \mathbb{R}^{h \times h} \quad (18)$$

$$\hat{y}^d = \text{SumPool}(V_d W^C + V_d W) \quad (19)$$

This replacement aims to improve the model's performance in handling imbalanced data by integrating information from both code description and original parameters. By implementing this change, we ensure that the more infrequent codes, which are often overlooked or inadequately represented in prior works, receive more attention.

3.5 Training

The training objective is to minimize the binary cross-entropy loss between the prediction \bar{y}^d and the target y , using the medical note d as training data. Additionally, we incorporate associated and hierarchical code descriptions to distill the medical note, capturing relevant medical words and the code hierarchy.

$$\text{Loss}(d, y) = - \sum_{i=1}^{N_L} (y_i \log \bar{y}_i^d + (1-y_i)(1-\log \bar{y}_i^d)) \quad (20)$$

$$L = \text{Loss}(d, y) + L_{ades} + L_{sdes} \quad (21)$$

4 Experiments

4.1 Datasets

In our study, we utilize the widely accessible MIMIC-III dataset (Johnson et al., 2016). MIMIC-III is an extensive, anonymized dataset comprising over 40,000 patient records from intensive care units at Beth Israel Deaconess Medical Center. It encompasses a diverse range of data, including laboratory measurements, vital signs, medications, and medical notes. Consistent with prior research, our primary focus is on predicting ICD codes for discharge summaries, where each note is linked to a specific hospital stay.

MIMIC-III discharge summaries are meticulously coded by professional coders with one or more ICD-9 codes, reflecting the diagnoses and procedures for each stay. The dataset encompasses 8,921 unique ICD-9 codes, subdivided into 6,918 diagnosis codes and 2,003 procedure codes. Notably, the dataset includes records of patients with multiple admissions, each associated with distinct discharge summaries. In alignment with earlier studies and to ensure uniform distribution of a patient’s notes across the training, validation, and test sets, we adopt the data split methodology proposed by (Mullenbach et al., 2018). The MIMIC-III dataset offers two primary configurations: the comprehensive MIMIC-III Full and the more focused MIMIC-III 50. The former includes all 8,921 codes and contains 47,719, 1,631, and 3,372 discharge summaries for training, development, and testing, respectively. The latter, MIMIC-III 50, encompasses the top 50 most frequent codes and includes 8,067, 1,574, and 1,730 discharge summaries for the respective phases.

4.2 Evaluation Metrics

Our evaluation approach is informed by the methodology of (Yuan et al., 2022), employing Micro and Macro AUC (area under the ROC curve), Micro and Macro F1 scores, and Precision@K as our primary metrics. For the MIMIC-III 50 dataset, we specifically report Precision@5 (P@5) and, for the comprehensive MIMIC-III Full, Precision@8 (P@8).

4.3 Baselines

We compare our method with the following baselines:

CAML (Mullenbach et al., 2018): A pioneering model in automated ICD coding, utilizing a

label attention layer for generating label-specific representations.

MultiResCNN (Li and Yu, 2020): This model leverages a multi-filter convolutional layer to capture diverse patterns in medical notes and a residual block to expand the model’s receptive field. It incorporates a label attention mechanism for creating label-specific representations.

LAAT (Vu et al., 2020): This model proposes a new label attention model to learn attention scores over BiLSTM encoding hidden states for each medical code.

Fusion (Luo et al., 2021): This model combines multi-CNN, Transformer encoder, and label attention to enhance performance and accuracy in ICD coding.

MSMN (Yuan et al., 2022): This model uses code synonyms collected from medical knowledge graph with adapted multi-head attention and LSTM encoder.

Rare-ICD (Chen et al., 2023): This model uses relations between different codes via a relation-enhanced code encoder to improve the rare code performance.

4.4 Implementation Details

We use word2vec to pre-train word embeddings with the size of 100 from medical notes and code description. Regarding the training of baseline models and their counterparts under the proposed MCDA framework, the optimizer and hyperparameters were kept consistent with the default parameter settings of the baseline models. For the MIMIC-III 50 configuration, training is conducted using a single 32GB NVIDIA-V100 GPU. In contrast, for the MIMIC-III Full setting, the training process utilizes two 32GB NVIDIA-V100 GPUs.

4.5 Results

Table 1 presents a comparison of performance between the baseline models and the proposed AHDD framework under both the MIMIC-III Full and MIMIC-III 50 settings.

Overall, it can be observed that the implementation of the AHDD framework enhances the performance of all baseline models. This demonstrates the effectiveness and necessity of distilling medical notes by associated and hierarchical code description. The significant improvement in F1 and Precision@K scores further substantiate the efficacy of the proposed framework in capturing relevant medical words for clinicians. Performance metrics,

Model	MIMIC-III Full					MIMIC-III 50				
	Auc		F1		P@8	Auc		F1		P@5
	Macro	Micro	Macro	Micro		Macro	Micro	Macro	Micro	
CAML	88.0	98.3	5.7	50.2	69.8	87.3	90.6	49.6	60.3	60.5
+AHDD	90.5	98.5	5.8	50.7	69.8	89.1	91.6	56.3	63.1	62.0
MultiResCNN	90.5	98.6	7.6	55.1	73.8	89.7	92.5	59.8	66.8	63.3
+AHDD	90.6	98.6	8.6	56.2	73.9	90.7	93.2	61.3	67.6	64.0
LAAT	91.9	98.8	9.9	57.5	73.8	92.5	94.6	66.1	71.6	67.1
+AHDD	94.7	99.1	10.2	57.9	74.7	92.5	94.6	67.8	71.7	67.3
Fusion	91.5	98.7	8.3	55.4	73.6	90.3	93.1	60.4	67.8	63.8
+AHDD	92.3	98.8	9.2	56.3	74.1	91.2	93.2	62.6	68.1	64.4
MSMN	95.0	99.2	10.3	58.2	74.9	92.7	94.6	67.4	71.7	67.4
+AHDD	95.0	99.2	10.4	58.8	75.3	92.8	94.7	68.5	72.8	67.8
Rare-ICD	94.7	99.1	10.5	58.1	74.5	91.9	94.2	64.2	70.8	66.5
+AHDD	95.2	99.3	10.9	58.9	75.3	92.1	94.3	65.8	71.3	66.8

Table 1: Results on the MIMIC-III Full and MIMIC-III 50 datasets.

particularly those focusing on the micro scale, provide insight into the effectiveness of addressing the issue of noisy text. Our AHDD framework accurately captures the representations of medical notes, a critical factor in dealing with noisy text scenarios.

To further validate this deduction, we have categorized medical notes into five distinct groups based on the average note length associated with label: [0,500], [501,1000], [1001,1500], [1501,2000], and [2001, +∞]. For each of these average note length groups, we computed the micro-averaged F1 score across all baseline methods and compared them to their counterparts within our AHDD framework. The summarized results are presented in Figure 3.

A notable observation from this analysis is the significant improvement in F1 scores that AHDD brings to the [0,500], [501,1000], [1001,1500], and [1501,2000] groups. Furthermore, these relative improvements become increasingly pronounced with the lengthening of the average medical note. This trend underscores the effectiveness of our AHDD framework in identifying key words within noisy and complex medical notes, validating its capability to handle such challenging data effectively.

For the MSMN model, the implementation of AHDD yields improvements in the [0,500], [501,1000], [1001,1500], and [1501,2000] groups. However, it exhibits a decline in performance in

the [2001, +∞] group. A plausible explanation for this could be that MSMN derives label-specific representations through multi-head attention. As the average length of the medical note increases, these representations are more likely to incorporate information pertaining to frequently occurring codes. Consequently, the decrease in F1 scores in the [2001, +∞] group could be attributed to MSMN’s tendency to assign these prevalent codes to longer medical notes.

To further corroborate this hypothesis, we also calculated the P@5 scores for MSMN in the [2001, +∞] group. Under the AHDD framework, an increase in the P@5 scores (17.5 of MSMN, 18.8 of MSMN+AHDD) is observed, suggesting that MSMN is indeed more prone to assign frequent codes to medical notes in this longer length group.

4.6 Ablation Study

To comprehensively assess the impact of each individual component, we carried out a series of ablation experiments on MSMN+AHDD. The results of these experiments are detailed in Table 2. From these results, it can be observed that:

Effectiveness of Associated Code Description Distillation When discarding the associated code description distillation (w/o ADD in Table 2), the performance drops dramatically in various metrics, especially on P@5 metric. It shows the effective-

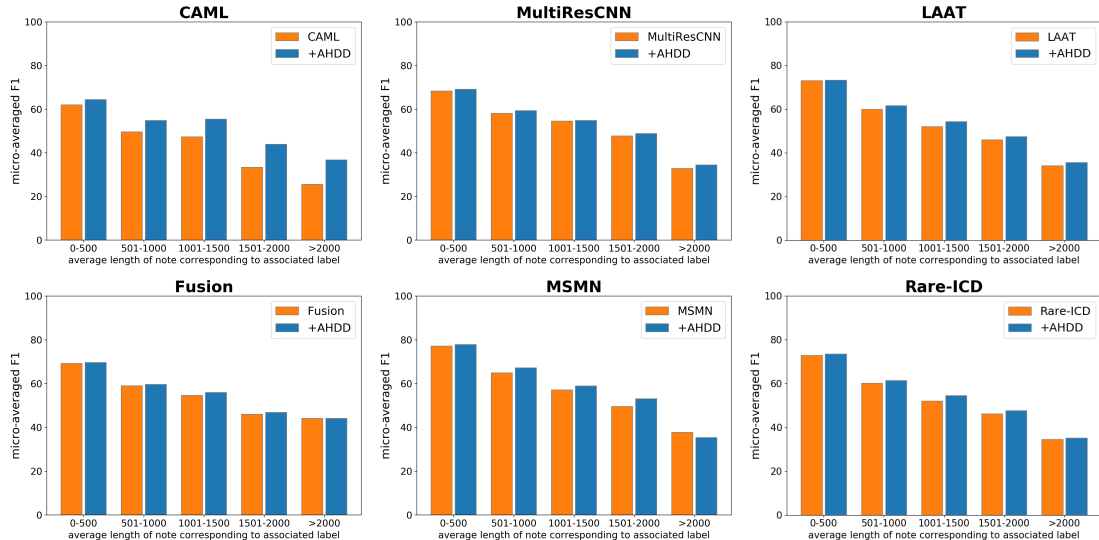


Figure 3: Micro-averaged F1 for the average note length groups associated with label for CAML, MultiResCNN, LAAT, Fusion, MSMN and Rare-ICD models. The x-axis represents the groups based on average note length, while the y-axis shows the micro-averaged F1 for each of these groups.

Model	Auc		F1		P@5
	Macro	Micro	Macro	Micro	
MSMN+AHDD	92.8	94.7	68.5	72.8	67.8
w/o ADD	92.8	94.7	68.0	72.2	67.5
w/o HDD	92.8	94.6	67.9	71.9	67.8
w/o D-att	92.8	94.7	68.5	72.3	67.7
w/o D-output	92.8	94.7	68.0	72.0	67.6

Table 2: Ablation results on the MIMIC-III 50 dataset.

ness of associated code description distillation in capturing key words in noisy and complex medical notes.

Effectiveness of Hierarchical Code Description Distillation When discarding the hierarchical code description distillation (w/o HDD in Table 2), the performance drops obviously in various metrics, especially on F1 metric. But the metric of P@5 keeps the same. It shows the effectiveness of hierarchical code description distillation in avoidance of inappropriate code assignments.

Effectiveness of Code Description Aware Attention Without Code Description Aware Attention (w/o D-att in Table 2), attention layers degrades to attention layers in previous works. The performance drops obviously in various metrics, especially on F1 and P@5 metric. It shows a significant reduction in the ability to capture important words.

Effectiveness of Code Description Aware At-

tention and Output Without Code Description Aware Output (w/o D-output in Table 2), output layers degrades to output layers in previous works. The performance drops obviously in various metrics, especially on F1 and P@5 metric. It shows a significant reduction in the ability to predict rare codes.

5 Conclusion

We propose a novel framework based on associated and hierarchical code description distillation to predict ICD codes. The code description is also applied to aware the attention layer and output layer. To the best of our knowledge, our work is the first attempt to use associated and hierarchical code descriptions for distilling medical notes. The framework is encoder-agnostic, and it neither needs extra text processing nor brings in too many parameters. The experimental results demonstrate that our proposed framework surpasses several leading state-of-the-art models on a benchmark dataset.

6 Limitation

Our proposed AHDD framework needs to calculate the the label-specific representation of the associated and hierarchical codes' description to distill the medical note during the training phase, thus we need a little more GPU resources and computational time. However, the need of resource occupancy and time consumption of our approach does not increase during inference.

Our framework is based on code description, a concise text lacking diversity. To further capture key words related to label description, more external knowledge will be incorporated to promote medical code prediction task.

References

- Biplob Biswas, Thai-Hoang Pham, and Ping Zhang. 2021. [Transicd: Transformer based code-wise attention model for explainable icd coding](#). In *Artificial Intelligence in Medicine*, pages 469–478, Cham. Springer International Publishing.
- Alex Bottle and Paul Aylin. 2008. [Intelligent information: a national system for monitoring clinical performance](#). *Health services research*, 43(1p1):10–31.
- Pengfei Cao, Yubo Chen, Kang Liu, Jun Zhao, Shengping Liu, and Weifeng Chong. 2020. [Hypercore: Hyperbolic and co-graph representation for automatic icd coding](#). In *Proceedings of the 58th Annual Meeting of the Association for Computational Linguistics*.
- Jiamin Chen, Xuhong Li, Junting Xi, Lei Yu, and Haoyi Xiong. 2023. [Rare codes count: Mining inter-code relations for long-tail clinical text classification](#). In *Clinical Natural Language Processing Workshop*.
- Edward Choi, Mohammad Taha Bahadori, Andy Schuetz, Walter F. Stewart, and Jimeng Sun. 2016. [Doctor ai: Predicting clinical events via recurrent neural networks](#). In *Proceedings of the 1st Machine Learning for Healthcare Conference*, volume 56 of *Proceedings of Machine Learning Research*, pages 301–318, Northeastern University, Boston, MA, USA. PMLR.
- Goncalo Gomes, Isabel Coutinho, and Bruno Martins. 2024. [Accurate and well-calibrated icd code assignment through attention over diverse label embeddings](#). In *Conference of the European Chapter of the Association for Computational Linguistics*.
- Alistair E.W. Johnson, Tom J. Pollard, Lu Shen, Liwei H. Lehman, Mengling Feng, Mohammad Ghassemi, Benjamin Moody, Peter Szolovits, Leo Anthony Celi, and Roger G. Mark. 2016. [Mimic-iii, a freely accessible critical care database](#). *Scientific Data*.
- Fei Li and Hong Yu. 2020. [Icd coding from clinical text using multi-filter residual convolutional neural network](#). *Proceedings of the AAAI Conference on Artificial Intelligence*, page 8180–8187.
- Junyu Luo, Xiaochen Wang, Jiaqi Wang, Aofei Chang, Yaqing Wang, and Fenglong Ma. 2024. [Corelation: Boosting automatic icd coding through contextualized code relation learning](#). *ArXiv*, abs/2402.15700.
- Junyu Luo, Cao Xiao, Lucas Glass, Jimeng Sun, and Fenglong Ma. 2021. [Fusion: Towards automated icd coding via feature compression](#). In *Findings of the Association for Computational Linguistics: ACL-IJCNLP 2021*.
- Julia Medori and Cédric Fairon. 2010. [Machine learning and features selection for semi-automatic ICD-9-CM encoding](#). In *Proceedings of the NAACL HLT 2010 Second Louhi Workshop on Text and Data Mining of Health Documents*, pages 84–89, Los Angeles, California, USA. Association for Computational Linguistics.
- James Mullenbach, Sarah Wiegrefe, Jon Duke, Jimeng Sun, and Jacob Eisenstein. 2018. [Explainable prediction of medical codes from clinical text](#). In *Proceedings of the 2018 Conference of the North American Chapter of the Association for Computational Linguistics: Human Language Technologies, Volume 1 (Long Papers)*.
- Kimberly J. O’Malley, Karon F. Cook, Matt D. Price, Kimberly Raiford Wildes, John F. Hurdle, and Carol M. Ashton. 2005. [Measuring diagnoses: Icd code accuracy](#). *Health Services Research*, 40(5p2):1620–1639.
- Adler Perotte, Rimma Pivovarov, Karthik Natarajan, Nicole Weiskopf, Frank Wood, and Noémie Elhadad. 2014. [Diagnosis code assignment: models and evaluation metrics](#). *Journal of the American Medical Informatics Association*, page 231–237.
- Elyne Scheurwegs, Boris Cule, Kim Luyckx, Léon Luyten, and Walter Daelemans. 2017. [Selecting relevant features from the electronic health record for clinical code prediction](#). *Journal of Biomedical Informatics*, 74:92–103.
- F.-C. Tsui. 2002. [Value of icd-9-coded chief complaints for detection of epidemics](#). *Journal of the American Medical Informatics Association*, 9(90061):41S – 47.
- Thanh Vu, Dat Quoc Nguyen, and Anthony Nguyen. 2020. [A label attention model for icd coding from clinical text](#). In *Proceedings of the Twenty-Ninth International Joint Conference on Artificial Intelligence*.
- Shilong Wang, Hongfei Lin, Yijia Zhang, Xiaobo Li, and Wen Qu. 2023. [Mkfn: Multimodal knowledge fusion network for automatic icd coding](#). *2023 IEEE International Conference on Bioinformatics and Biomedicine (BIBM)*, pages 2294–2297.
- Tao Wang, Linhai Zhang, Chenchen Ye, Junxi Liu, and Deyu Zhou. 2022. [A novel framework based on medical concept driven attention for explainable medical code prediction via external knowledge](#). In *Findings of the Association for Computational Linguistics: ACL 2022*, pages 1407–1416, Dublin, Ireland. Association for Computational Linguistics.
- Jing Xie, Xin Li, Ye Yuan, Yi Guan, Jingchi Jiang, Xitong Guo, and Xin Peng. 2024. [Knowledge-based](#)

dynamic prompt learning for multi-label disease diagnosis. *Knowledge-Based Systems*, 286:111395.

Pengtao Xie and Eric Xing. 2018. A neural architecture for automated icd coding. In *Proceedings of the 56th Annual Meeting of the Association for Computational Linguistics (Volume 1: Long Papers)*.

Zheng Yuan, Chuanqi Tan, and Songfang Huang. 2022. Code synonyms do matter: Multiple synonyms matching network for automatic ICD coding. In *Proceedings of the 60th Annual Meeting of the Association for Computational Linguistics (Volume 2: Short Papers)*, pages 808–814, Dublin, Ireland. Association for Computational Linguistics.

Tong Zhou, Pengfei Cao, Yubo Chen, Kang Liu, Jun Zhao, Kun Niu, Weifeng Chong, and Shengping Liu. 2021. Automatic icd coding via interactive shared representation networks with self-distillation mechanism. In *Proceedings of the 59th Annual Meeting of the Association for Computational Linguistics and the 11th International Joint Conference on Natural Language Processing (Volume 1: Long Papers)*.

A Appendix

A.1 Case Study

Medical Note: The patient was taken for an ERCP the day after admission, where he was found to have a stone in the common bile duct treated with sphincterotomy and stone extraction. He was treated with broad spectrum antibiotics. Following the ERCP, he then **appeared to bleed** from his sphincterotomy. His **initial hematocrit** was 40 and it then fell to 25. He received 2 units of **transfusion**. He was then stable after that.

(Fusion)

Medical Note: The patient was taken for an ERCP the day after admission, where he was found to have a stone in the common bile duct treated with sphincterotomy and stone extraction. He was treated with broad spectrum antibiotics. Following the ERCP, he then **appeared to bleed** from his sphincterotomy. His **initial hematocrit** was 40 and it then fell to 25. He received 2 units of **transfusion**. He was then stable after that.

(Fusion+AHDD)

ICD-9 code:285.1(Acute posthemorrhagic anemia)

Figure 4: The attention distribution visualization over a medical note with a medical code for Fusion and its counterparts under AHDD framework. We calculate the attention score over hidden states encoded, and highlight the highly weighted words.

Visualization of Attention Distribution To further explore the proposed framework’s ability to capture relevant information, we present a visualization of the attention distribution over a medical note. This visualization compares Fusion and its counterparts within our AHDD framework, as illustrated in Figure 4.

It can be observed that Fusion only captures scattered label-related words like "appeared to", "initial hematocrit" and "transfusion" for inferring "anemia", while it fails to find valid relevant evidence for inferring "Acute posthemorrhagic anemia". In contrast, the AHDD framework, which utilizes associated and hierarchical code description distillation, successfully identifies the crucial word "bleed" to infer ICD code 285.1. Therefore, through the distillation, the model can more effectively capture significant words and avoid improper code assignments.

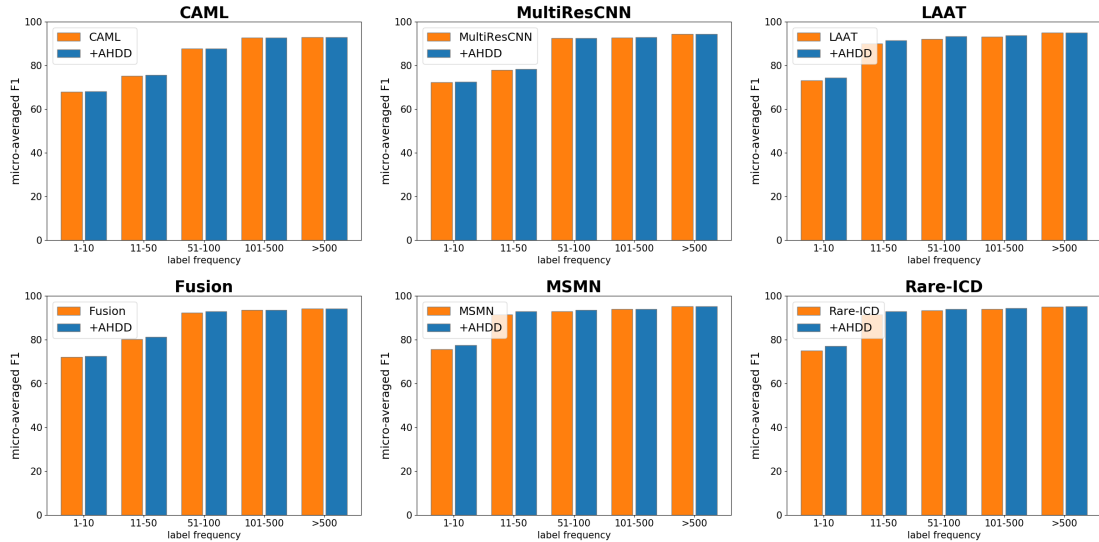


Figure 5: Micro-averaged F1 for the label frequency groups for CAML, MultiResCNN, LAAT, Fusion, MSMN and Rare-ICD models. The x-axis represents the groups based on label frequency, while the y-axis shows the micro-averaged F1 for each of these groups.

A.2 Experiment About Rare Codes

The proposed method also addresses the issue of rare codes. We have adopted the data split methodology proposed by (Wang et al., 2022), dividing medical codes into five groups: [1,10], [11,50], [51,100], [101,500], and [501, $+\infty$] based on frequency in the dataset and calculating the macro-averaged F1 for each group. The results, as summarized in Figure 5., demonstrate the effectiveness of our method across different frequency groups.

A.3 Ablation Study On Other Methods

To comprehensively assess the impact of each individual component, we carried out a series of ablation experiments on other methods. The results of these experiments are detailed in Table 3.

model	Auc		F1		P@5
	Macro	Micro	Macro	Micro	
CAML+AHDD	89.1	91.6	56.3	63.1	62.0
w/o ADD	89.0	91.5	56.2	63.1	61.8
w/o HDD	89.0	91.6	56.2	63.1	62.0
w/o D-att	88.3	90.9	56.0	63.0	61.8
w/o D-output	89.0	91.6	56.1	63.1	61.6
MultiresCNN+AHDD	90.7	93.2	61.3	67.6	64.0
w/o ADD	90.7	93.2	60.4	67.5	63.6
w/o HDD	90.6	93.2	61.2	67.5	63.6
w/o D-att	90.5	93.1	60.8	67.6	63.9
w/o D-output	90.4	93.0	60.7	67.4	63.8
LAAT+AHDD	92.5	94.6	67.8	71.7	67.3
w/o ADD	92.5	94.6	67.8	71.2	67.2
w/o HDD	92.5	94.6	67.8	71.4	67.2
w/o D-att	92.1	94.2	66.5	70.6	66.3
w/o D-output	92.0	94.1	66.7	70.7	66.0
Fusion+AHDD	91.2	93.2	62.6	68.1	64.4
w/o ADD	91.1	93.2	61.4	67.5	64.3
w/o HDD	91.1	93.2	62.4	68.0	64.4
w/o D-att	91.0	93.1	62.6	67.9	63.9
w/o D-output	91.0	93.0	62.5	67.9	64.0
Rare-ICD+AHDD	92.1	94.3	65.8	71.3	66.8
w/o ADD	92.1	94.3	64.3	70.3	66.1
w/o HDD	91.9	94.2	65.2	70.9	66.1
w/o D-att	91.9	94.3	65.1	71.0	66.0
w/o D-output	91.0	94.0	65.5	70.9	66.0

Table 3: Ablation results on other methods on the MIMIC-III 50 dataset.